Technical Paper

ISSN 1997-1400 Int. J. Pavement Res. Technol. 4(1):21-33

Evaluation of the CalME Permanent Deformation Model for Asphalt Concrete Layers

Erik Oscarsson[1+] and Lorina Popescu[2]

Abstract: This paper presents an evaluation of the model for permanent deformation in asphalt concrete layers used in the CalME incremental-recursive mechanistic-empirical method. The permanent deformation modeling was carried out using the CalME software v0.82 in two pavement test sections on the E6 motorway at Fastarp-Heberg, Sweden. The measured traffic, material and climate input data were in some instances completed by CalME default material data. The results indicate that the relation between plastic and elastic shear properties, derived with the Repeated Simple Shear Test at Constant Height, may be affected by ageing. The suggested main ageing effect is loss of dependency on the number of loadings. The model results using default permanent deformation material data correlated well with field measurements in the flexible pavement section. The results from the semi-rigid pavement section indicate that shear stress and elastic shear strain may be difficult to relate to flow rutting in very stiff pavement sections.

Key words: *Asphalt concrete, Flow rutting, CalME, Permanent deformation, Model.*

Introduction

Rutting due to permanent deformation is considered one of the most serious distress mechanisms in asphalt pavements. It causes traffic hazards by affecting vehicle steering. Further, an impervious road surface will trap water, snow and ice that cause hydroplaning and loss of friction. Longitudinal cracks sometimes occur in deep ruts where they drain free water into the underlying pavement layers, thereby increasing the deterioration rate. The factors affecting permanent deformations can be divided into traffic loading, material properties and climatic conditions.

Modeling is a valuable tool used for pavement design and residue assessment. The first pavement deterioration models were entirely empirical but mechanistic principles have been introduced over the last years. In California, three methodologies are currently employed in the Caltrans mechanistic-empirical software v0.82, known as CalME [1]. The first, called the Hveem methodology, empirically designs layer thicknesses using the R-value method by Caltrans [2]. The second, called the Classical mechanistic-empirical design methodology, employs linear elastic multilayer analysis using a single representative temperature and the dual wheel equivalent standard axle load (ESAL) of 80 kN uniformly distributed with a 0.69 MPa contact pressure. The response functions that determine the permissible number of ESALs are based on the Asphalt Institute criteria by default.

The third and most advanced CalME methodology, evaluated in this study, is called the incremental-recursive mechanistic-empirical model. Incremental-recursive modeling means that the analysis is divided into increments, and the results of each increment are used as input in the next. The mechanistic-empirical modeling is based on linear elastic multi-layer theory combined with a number of distress functions. The CalME incremental-recursive mechanistic-empirical model will be referred to as the CalME model hereafter in this paper. CalME has some similarities with the Mechanistic-Empirical Pavement Design Guide (M-E PDG) model developed by NCHRP [3] including consideration of the most important distress mechanisms, i.e. cracking and rutting. Two major differences are that CalME was primarily designed for rehabilitation and pavement preservation design, and the incremental-recursive form of the damage models. It should be noted that this study was limited to rutting.

The analysis is divided into finite increments, where each month is represented by its middle day by default. Each day is then divided into five periods in which each sublayer temperature is assumed constant [4]. The CalME temperature profile is modeled with an incremental-recursive one-dimensional finite element subroutine using hourly surface temperature and a constant deep soil temperature. The hourly surface temperature is normally pre-calculated with the Enhanced Integrated Climate Model (EICM) [5].

In each increment, stresses and elastic strains are modeled with linear elastic multi-layer theory using heavy vehicle load spectra derived with weigh-in-motion (WIM). The elastic material input data are based mainly on field tests such as back-calculation using Falling Weight Deflectometer (FWD) deflections, or frequency sweep testing performed with cored specimens.

The permanent deformation in asphalt concrete is modeled using a shear strain function similar to some previous modeling efforts [6, 7]. The plastic shear strain is modeled as a function of the shear stress at 50 mm depth below the outer tire edge, the permanent shear strain in each sublayer, and laboratory-determined coefficients from the Repeated Simple Shear Test at Constant Height (RSST-CH). The flow rutting is assumed to be proportional to asphalt concrete depth down to 100 mm. The current version of CalME is calibrated using Heavy Vehicle Simulator (HVS) tests and observations at WesTrack [8, 9]. Recent work has extended this approach to calculate rutting

[1] Department of Technology and Society, Faculty of Engineering, Lund University, Sweden. Box 118, 221 00 Lund, Sweden.
[2] Pavement Research Center, Institute of Transportation Studies, University of California, Berkeley, USA, 1353 S 46th St, Building 452-T, Richmond CA 94804-4603, USA.
[+] Corresponding Author: E-mail erik.oscarsson@skanska.se
Note: Submitted March 2, 2010; Revised May 7, 2010; Accepted May 24, 2010.

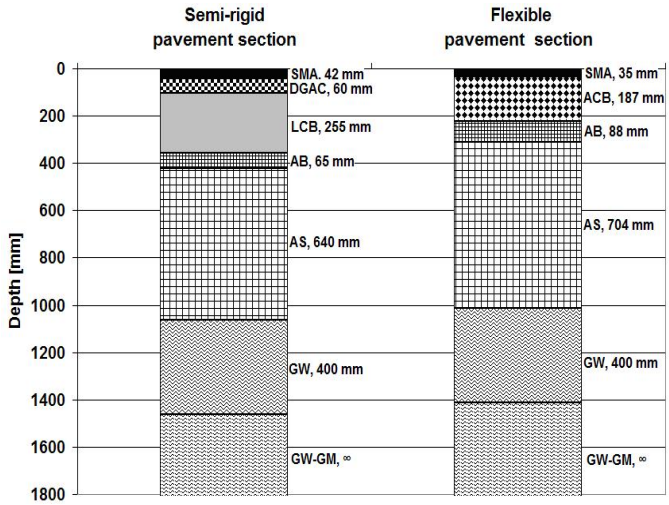

Fig. 1. The Pavement Structure of the Test Sections.

within the top 100 mm of the pavement when there are different asphalt layers with very different properties, such as conventional asphalt overlaid with rubber asphalt or heavily modified mixes [10].

Methods

Permanent deformation modeling was carried out for two test sections on the E6 motorway at Fastarp-Heberg, Sweden. The observed semi-rigid and flexible pavement test sections were opened for traffic in November 1996. The study focused on specific transversal sections, rather than mean values over distances, which would cause variations in rut depth and material properties. Pavement test sections exhibiting heavy rutting were preferred over well preserved sections in order to minimize the relative measurement error. Therefore, the measured rut depth data and material properties of a specific section are not necessarily representative for all sections of the project.

Structure and Materials

The structure and materials data of the semi-rigid and flexible pavement test sections were input primarily using measured data and completed with default WesTrack material data. Only measured data should ideally be used to reach the highest accuracy and to benefit from the mechanistic model considerations. However, all tests that are normally carried out to define the CalME material parameters could not be performed. This was due to a lack of asphalt concrete specimens caused by field coring limitations. Therefore, the input data most important to rutting were measured. The measured data were completed with data from a reference material that was estimated for each of the asphalt concrete, aggregate base and subgrade materials. Each reference material was calculated as the mean corresponding parameter from the WesTrack sections 01 to 04 and 14 to 18. Those sections constituted the majority of the current WesTrack calibration sections with materials available in the CalME software materials library. The WesTrack asphalt concrete (AC) materials included varying asphalt binder content and air void content, but only fine aggregates. However, it should be noted that the sections with fine aggregate AC exhibited better rutting resistance than the sections with coarse aggregate AC [9]. More information on the complete material data set is provided in the CalME manual [4].

Modeling was carried out using both measured and alternative default asphalt concrete (AC) permanent deformation parameters. The data measured in this study were based on a limited number of specimens due to field coring limitations at the E6 motorway in Sweden. Therefore, comparison with simulation results using default CalME material data appeared necessary. The default AC permanent deformation data were defined as the mean data from the WesTrack sections 01 to 04 and 14 to 18 [9]. The default approach can be considered equivalent to using the M-E PDG at Level 3. Future versions of CalME with regional material libraries are expected to increase model accuracy.

The semi-rigid pavement section 9:22 was constructed with a 42 mm stone mastic asphalt (SMA) with penetration 70/100 bitumen, 60 mm dense-graded asphalt concrete (DGAC) with penetration 70/100 bitumen, 255 mm lean concrete base (LCB), 65 mm aggregate base (AB), 640 mm aggregate subbase (AS), 400 mm well-graded gravel (GW) subgrade and a semi-infinite well-graded/silty gravel (GW-GM) subgrade layer, as presented in Fig. 1. The flexible pavement section 10:7 was constructed with 35 mm SMA with penetration 70/100 bitumen, 187 mm asphalt concrete base (ACB) layer with penetration 160/220 bitumen, 88 mm AB, 704 mm AS, 400 mm GW and a semi-infinite GW-GM layer. Further details on the E6 Fastarp-Heberg pavement test sections are provided in the construction documentation [11, 12]. All layers were input separately, as the CalME software is capable of modeling an infinite number of layers [4].

Asphalt Concrete Layers

The asphalt concrete properties directly affecting permanent deformation were measured while other data were estimated using mean data from WesTrack asphalt concrete materials. Full-depth field cores with diameter 150 mm were obtained from each of the semi-rigid and flexible test sections in May 2008, i.e. 11.5 years after pavement construction. The cores were obtained from between the wheel tracks, i.e. an area largely unaffected by traffic loadings. Therefore, the cores were considered to be affected by ageing but not by damage due to traffic loadings. The upper portion of each layer in each core was cut to specimens with a 150 mm diameter and a height of 40-50 mm, depending on the layer thickness. The SMA wearing layer of the flexible section cores was not tested due to an average thickness of less than 40 mm. Instead, the results from the theoretically identical semi-rigid section SMA specimens were used for both sections.

Ageing

The ageing properties of the asphalt concrete materials were defined using the Swedish specifications to provide the CalME software with input data and to age-adjust the dynamic modulus data derived from cored specimens. The constants of the CalME ageing function, presented in Eq. (1), were determined using a predefined ageing function, shown in Eq. (2), according to Swedish specifications [13] based on an ageing study [14].

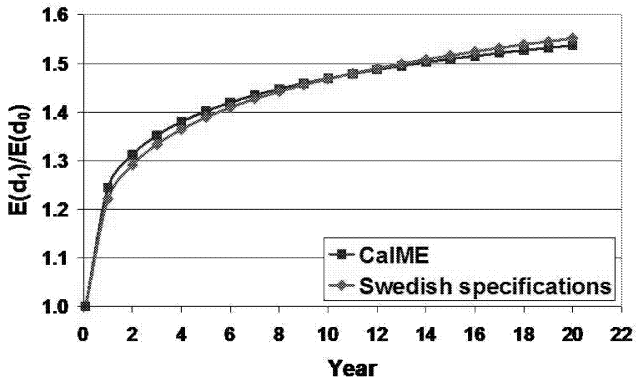

Fig. 2. The CalME and the Swedish Specifications Ageing Functions.

$$E(d_1) = E(d_0)\frac{A_{age} \times \ln(d_1) + B_{age}}{A_{age} \times \ln(d_0) + B_{age}} \quad (1)$$

$$E(d_0) = E(d_1)\frac{1.313}{d_1^{0.08}} \quad (2)$$

where
E: Dynamic modulus [MPa].
d_0: Initial age [days].
d_1: Current age [days].
A_{age}, B_{age}: Constants.

The Swedish specifications requirement of d_0 = 30 days was assumed. Eqs. (1, 2) were rearranged to express the ageing ratio $E(d_1)/E(d_0)$. The current modulus at any time can then be calculated as the product of the ageing ratio and the initial modulus. The ageing ratios were then converged by adjusting the CalME constants to find the minimum sum of squared errors. The constants A_{age} = 1.00 and B_{age} = 6.83 resulted in a good curve fit throughout the expected pavement life, as illustrated in Fig. 2. The ageing ratio for adjustment of dynamic modulus and measured asphalt concrete permanent deformation data derived with 11.5 years old cores was 1.48. The estimated initial age of all layers at traffic opening was 90 days based on the construction documentation [11].

Dynamic Modulus Data

The asphalt concrete dynamic modulus input data were obtained using frequency sweeps on field cores in indirect tensile test (IDT) mode [15]. Three replicate specimens from each layer type were subjected to indirect tensile haversine loading cycles at the temperatures -10°C, 5°C, 20°C and 35°C. At each temperature, a frequency sweep was carried out using the frequencies 25, 20, 10, 5, 2, 1, 0.5, 0.2 and 0.1 Hz. At each frequency, ten preconditioning pulses were applied, followed by ten test pulses. No 0.01 Hz test at 35°C was carried out in order to minimize the risk of plastic specimen deformation and invalid test results. The temperature accuracy was ±0.5°C as measured with a dummy specimen integrated thermometer. The strain level range was 40-60 microstrain in order to receive a clear response signal while keeping within the linear viscoelastic range.

The mastercurves were constructed according to the sigmoidal function using frequency sweep data, the previously discussed 11.5 year ageing adjustment and the CalME minimum dynamic modulus assumption. The CalME sigmoidal function, defined with Eqs. (3) to (6) was based on the M-E PDG format [3, 4]. The assumption of a minimum dynamic modulus is supported with falling weight deflectometer measurements and motivated with the differences in boundary conditions of the specimen in a laboratory test compared to the field [8]. Further, the CalME manual [4] argues that the minimum dynamic modulus should at least correspond to the aggregate alone even though it may not fit frequency sweep data at the low stiffness end of the curve corresponding to high temperatures and low frequencies. Regardless of whether a minimum dynamic modulus assumption is correct or not in a generic sense, it was used in this paper since the model relies on it.

$$\log(|E^*|) = \delta + \frac{\alpha}{1 + e^{(\beta + \gamma \log(t_r))}} \quad (3)$$

$$t_r = t_l \times \left(\frac{\eta_{ref}}{\eta}\right)^{a_T} \quad (4)$$

$$t_l = \frac{1}{2 \times \pi \times f} \quad (5)$$

$$\log(\log(\eta)) = A + VTS \times \log(T_K) \quad (6)$$

where
$|E^*|$: Dynamic modulus [MPa].
δ: Constant.
α, β, γ: Constants determined using the least square error method.
t_r: Reduced time [s].
t_l: Loading time [s].
f: Loading frequency [Hz].
η_{ref}: Binder viscosity at reference temperature [cP].
η: Binder viscosity at current temperature [cP].
a_T: Constant for mastercurve.
A, VTS: Constants for binder viscosity.
T_K: Temperature [K]

The age-adjusted frequency sweep data resulted in a minimum

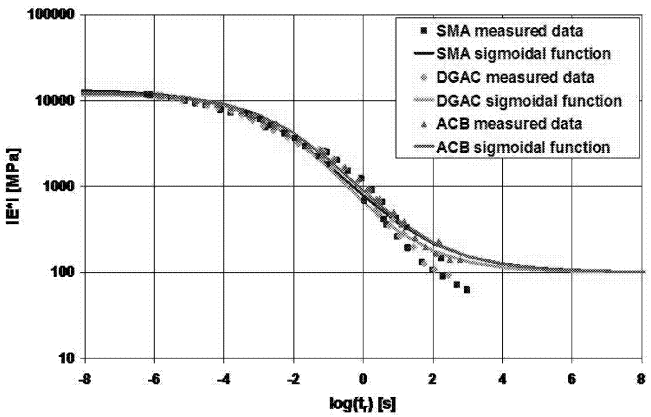

Fig. 3. Dynamic Modulus Test Data and Their Sigmoidal Functions.

Table 1. Mastercurve Parameters.

Test section	Asphalt Concrete Designation	$\|E^*\|_{ref}$ [MPa]	T_{ref} [°C]	v	α	β	γ	δ	a_T	A	VTS
Semi-rigid	SMA Wear Course	6053	12.5	0.35	2.1146	-0.3294	0.7397	2.0000	2.5890	10.0410	-3.6800
	DGAC Binder Course	5644	12.5	0.35	2.1038	-0.2747	0.7289	2.0000	2.4670	10.0410	-3.6800
Flexible	SMA Wear Course	6093	12.4	0.35	2.1146	-0.3396	0.7397	2.0000	2.5890	10.0410	-3.6800
	ACB Course	6176	12.4	0.35	2.1365	-0.4033	0.6805	2.0000	2.4885	10.0410	-3.6800

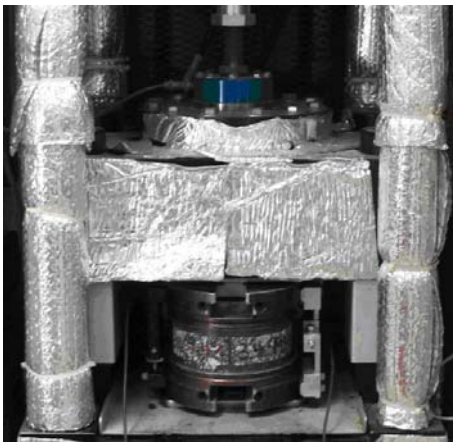

Fig. 4. The RSST-CH Device.

Fig. 5. A Shear Test Specimen Glued to Loading Platens.

dynamic modulus of somewhat less than 100 MPa for all asphalt materials. However, the CalME WesTrack calibration was based on a minimum modulus of 100 MPa [9] and the CalME manual recommends 100-200 MPa [4]. Therefore, the minimum dynamic modulus was assumed to be 100 MPa. The resulting mastercurve, derived with the least squared error sum method, and the age-adjusted measured data are illustrated in Fig. 3 and its parameters are presented in Table 1. It was noted that the measured and modeled dynamic moduli in Fig. 3 differ at low moduli, which is acceptable according to the previously discussed minimum dynamic modulus assumption. The reference dynamic modulus ($|E^*|_{ref}$) is defined with a 0.015 s loading time at the reference temperature (T_{ref}), i.e. the yearly mean surface temperature further discussed in the climate section. The default CalME asphalt materials Poisson's ratio of 0.35 and binder properties A = 10.0410 and VTS = -3.6800 were assumed for all asphalt materials. It should be noted that the constructed mastercurve is insensitive to the selection of binder properties [4].

Permanent Deformation Characteristics

Two sets of asphalt concrete permanent deformation parameters were derived for each material by using repeated simple shear test at constant height (RSST-CH) measurements and by assessing mean dense-graded asphalt concrete data from the WesTrack sections 01 to 04 and 14 to 18. The measured plastic strain data were fitted using the gamma function in Eq. (7). The latest version of CalME [1] models the corresponding flow rutting with Eqs. (7) and (9). The WesTrack permanent deformations parameters in the CalME material database are characterized with the previously used power function in Eq. (8). Consequently, CalME flow rutting calculations with WesTrack parameters employ Eqs. (8) and (9). It should be noted that the parameters in the gamma and power functions are not interchangeable.

$$\gamma_p = \exp\left(A + \alpha \times \left[1 - \exp\left(\frac{-\ln(N)}{\gamma}\right) \times \left(1 + \frac{\ln(N)}{\gamma}\right)\right]\right) \times \exp\left(\frac{\beta \times \tau}{\tau_{ref}}\right) \times \gamma_e^{\delta} \tag{7}$$

$$\gamma_p = A \times \left(N \times 10^{-6}\right)^{\alpha} \times \exp\left(\frac{\beta \times \tau}{\tau_{ref}}\right) \times \gamma_e^{\delta} \tag{8}$$

$$r_d = K \times h_i \times \gamma_p \tag{9}$$

where

r_d: Rut depth in asphalt concrete layers [mm].
K: Constant relating permanent shear strain to rut depth.
h_i: Layer thickness (down to 100mm depth) [mm].
γ_p: Plastic shear strain [MPa].
γ_e: Elastic shear strain [MPa].
τ: Shear stress [MPa].
τ_{ref}: Reference shear stress (0.1 MPa ≈ atmospheric pressure).
N: Number of load repetitions.
A, α, β, γ, δ: Constants determined using RSST-CH data.

The measured data sets were produced with the RSST-CH device shown in Fig. 4, by using specimens glued to loading platens [16],

Table 2. The RSST-CH Testing Conditions.

		Temperature [ºC]	
		40	50
Stress [kPa]	70	SMA, DGAC, ACB	SMA
	130	SMA, DGAC	DGAC, ACB

Table 3. Permanent Deformation Parameters.

	Material Name	A	α	β	γ	δ	τ_{ref}	K
Measured Data(Gamma Function)	SMA Wear Course	-0.467	3.652	1.03	1.517	1	0.1	0.08
	DGAC Binder Course	-0.5	4.204	1.03	1.252	1	0.1	0.08
	ACB Course	-0.383	4.276	1.03	1.49	1	0.1	0.08
Mean WesTrack Data (Power Function)	All Mix Types	14.073	0.129	1.03	1	1	0.1	0.9

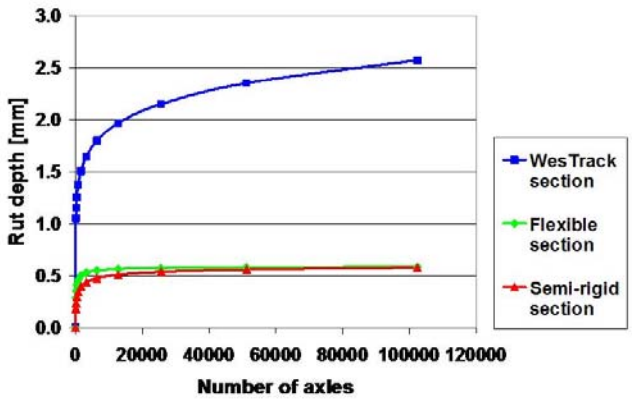

Fig. 6. Example of Permanent Deformation in Asphalt Concrete Layers.

Table 4. FWD Measured Median Modulus for Asphalt and Cement Bound Layers.

Year	1997	1998	1999	2001	2003
Pavement Temperature [°C]	8	12	4.5	13	8
Modulus [MPa]	19,500	18,600	18,400	17,500	13,000
Modulus at 10°C [MPa]	17,340	20,917	13,323	20,870	11,560

as illustrated in Fig. 5. The resulting permanent deformation parameters that define the relation between elastic and plastic strains are assumed constant throughout the pavement life [4]. The resulting permanent deformation parameters were based on a limited number of valid specimens: 3 for the stone mastic asphalt layer (SMA), 3 for dense-graded asphalt concrete (DGAC) layer and 2 for the asphalt concrete base (ACB) layer. The specimens were tested at different temperatures and stress levels as presented in Table 2. The limited number of specimens made it interesting to carry out additional simulations using corresponding CalME default data. This alternative asphalt concrete permanent deformation parameter set was obtained by calculating mean parameter values from the WesTrack sections 01 to 04 and 14 to 18 [9], which were characterized in the power function format. The resulting permanent deformation parameters from measurements and calculation are presented in Table 3.

An example of the effect of permanent deformation parameters on flow rutting in the test sections is illustrated in Fig. 6 under the assumptions $\tau = \tau_{ref}$, γ_e = 1000 microstrain and layer thicknesses according to Fig. 1. An imaginary asphalt concrete (AC) slab with mean WesTrack permanent deformation parameters appears to have almost 5 times higher the flow rutting potential than the AC layers in the semi-rigid and flexible pavement sections in this study. The semi-rigid and flexible pavement sections appear to have similar flow rutting potential. Further, the shape of the apparent flow rutting using the measured data differed from that of the mean WesTrack data. After the initial high increase, the measured flow rutting stabilized while the WesTrack curve showed a constant increase. However, it should be noted that these observations are based on the assumption of constant elastic strains.

Lean Concrete Base Layer

The modulus of the lean concrete base (LCB) layer in the semi-rigid pavement was measured using a falling weight deflectometer (FWD) on the pavement surface at the time of construction. All FWD measurement was carried out at temperatures close to the mean yearly surface temperature of 12.5°C. The measured modulus of the combined asphalt and cement bound layers was 19,500 MPa, which was considerably higher than intended [17] and almost twice as high as the 10,000 MPa CalME default LCB modulus. However, the high modulus FWD measurement is supported by the cored specimen compressive strength of 18.3 MPa [11] being more than twice as high as the 8.5 MPa recommended by Swedish specifications [18] at the time of construction. Therefore, the LCB modulus was estimated at 19,500 MPa.

The damage rate of the LCB material was assessed using repeated follow-up FWD measurements. This was necessary as no CalME cemented base materials were calibrated at the time of analysis. The documented back-calculated moduli of the combined asphalt and cement bound layers [17] are presented in Table 4. The moduli were normalized to 10°C using the modeled modulus ratio, where each component is assessed with Eq. (10) [6]. The results are also presented in Table 4.

$$E = \exp(A_0 + A_1 T) \tag{10}$$

where
E: E-modulus [MPa].
A_0 = 15.30039.
A_1 = -0.0587.
T: Temperature [°C].

A linear damage rate was estimated using the FWD data and CalME crushing parameters were calibrated accordingly. The linear degradation rate was determined by minimizing the sum of squared errors compared to the temperature-normalized modulus in Table 4. The resulting expression was E = (19500 – 780t) MPa, where t is traffic time in years. This corresponds to a 50% reduction of the

initial modulus after 12.5 years. Damage, i.e. loss of modulus, of cement bound materials was characterized using the crushing function in Eq. (11) [4]. The parameter values $\alpha = 1$, $\beta = 0$ and $\gamma = 0$ were assumed in order to obtain a close to constant rate damage function. Parameter $A = 0.0184$ was then assessed using trial and error in order to reach the 50% loss of modulus over 12.5 years.

$$\omega = A \times \left(\frac{N}{10^6}\right)^{\alpha} \times \left(\frac{\sigma}{\sigma_{ref}}\right)^{\beta} \times \left(\frac{E}{E_{ref}}\right)^{\gamma} \quad (11)$$

where
ω: Damage ratio ranging from 0 to 1
N: Number of load repetitions
σ: Vertical stress on top of layer [MPa]
σ_{ref}: Reference vertical stress on top of layer [MPa]
E: E-modulus adjusted for climate and damage [MPa]

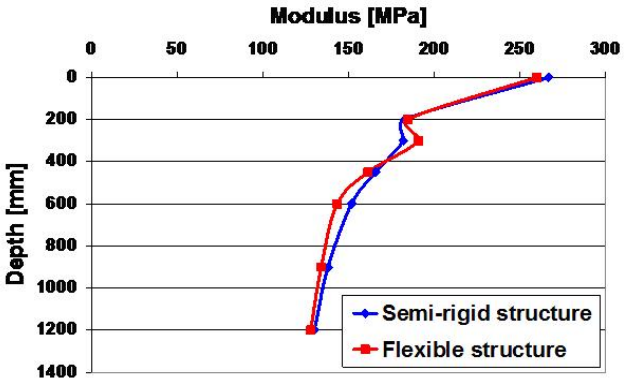

Fig. 7. FWD Moduli from the Aggregate Base Layer Top.

Table 5. Unbound Material Modulus Data.

Layer	Modulus [MPa]
Aggregate Base	223
Aggregate Subbase	180
Coarse-grained Subgrade	137
Fine-grained Subgrade	129

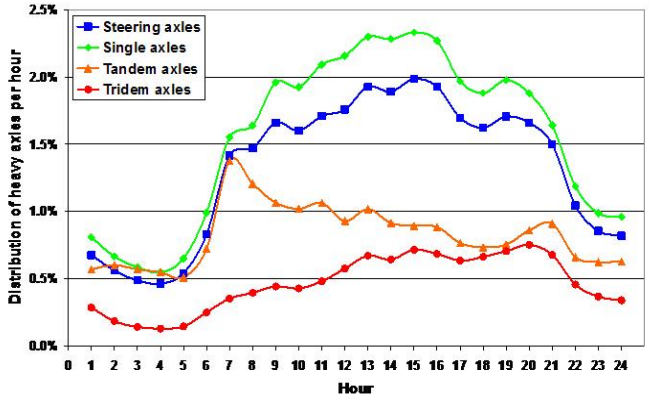

Fig. 8. Distribution of Heavy Axles throughout the Day.

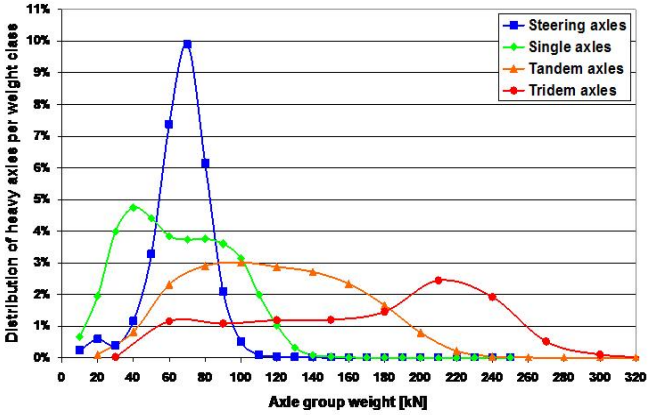

Fig. 9. Distribution of Heavy Axles per Weight Class.

E_{ref}: Reference modulus [MPa]
A, α, β and γ: Constants

The CalME permanent deformation parameters for the LCB were set according to the M-E PDG assumption that this mechanism is non-existent in chemically stabilized materials [3]. However, it should be noted that permanent deformation from underlying unbound materials can still manifest itself as rutting on the pavement surface in the CalME simulation. Remaining parameters were assumed to be those of the default CalME lean concrete base material.

Unbound Layers

The unbound layers were characterized using FWD data at the project that was completed by default aggregate base material data from the WesTrack sections. The modulus was estimated using FWD deflection data from measurements on the aggregate base layer during construction [12] and the mean modulus method [19]. The resulting moduli in the sections are very similar as shown in Fig. 7. This was expected since the unbound layers in both sections are theoretically identical and the unbound material layer thicknesses are similar. Therefore, each material was assigned a single constant modulus as presented in Table 5.

Traffic

The heavy axle load spectra and the number of heavy vehicles were measured with Weigh-in-motion (WIM) equipment and on-site pneumatic tubes or inductive loops that were stationary mounted on the pavement surface. The available one-week early summer WIM measurements were carried out in 2004 near Kungsbacka and 2005-2007 near Löddeköpinge [20]. These locations are 95 km north and 130 km south from the test sections, respectively. The heavy vehicle load spectra in Kungsbacka and Löddeköpinge were considered similar enough to allow interpolation of data.

CalME uses the assumption of constant axle load spectrum from year to year, over the week and throughout the day. Further, the axle load distribution is also assumed constant from month to month. The assumptions appear reasonable as very small seasonal load spectra variation has been reported in California despite the addition of agricultural transports during harvest time [21]. The distribution

of heavy vehicle axles at each hour throughout the day was assessed using the WIM data presented in Fig. 8. The WIM data also determined the axle weight distribution shown in Fig. 9. Quad axles constituted 0.02% of the total number of axles. Since they are not modeled by CalME, they were approximated as tridem axles.

The number of heavy vehicles measured with pneumatic tubes and inductive loops [22] was adjusted using the more detailed WIM data in order to exclude light vehicles with long axle spacing. The resulting number of axles during the first year was 1 126 000 and the yearly mean compound growth was 5.21%. The speed calculated using WIM data was 88.7 km/h (55.1 mph), as presented in Table 6. CalME calculates either the tire-to-pavement contact stress using the current load and a constant contact area, or the area using the load and a constant contact pressure, which normally is assumed equal to the tire inflation pressure. The former routine is normally preferred as it significantly reduces computation time. However, a typical contact area could not easily be assessed in this study, and CalME was largely calibrated using a constant 690 kPa inflation pressure [9] corresponding to the Californian Equivalent Standard Axle Load (ESAL). Therefore, an inflation pressure of 800 kPa was used, corresponding to the Swedish specifications ESAL [13]. Further, the CalME default option of modeling all non-steering axle tires as dual tires was employed because the use of super single tires in Sweden could not be assessed. However, it is known that super single tires are becoming more common and that they cause significantly more damage to asphalt concrete pavements than dual tires [23, 24]. Therefore, the increased damage due to the use of super single tires also motivates the higher-than-normal 800 kPa inflation pressure. The lateral wander average standard deviation of 290 mm was estimated using previous measurements [25] and the 3.5 m lane width. The results were inserted directly into the CalME traffic load database file.

Table 6. General Traffic Input Data.

Axles First Year	1 126 000
Growth Rate	5.21%
Speed	88.7 km/h
Contact Pressure	800 kPa
Wander Standard Deviation	290 mm

Table 7. EICM Output Data Summary.

Longitude, Latitude	12.46E, 56.47N
Elevation	18 m
Annual Water table Depth	2.2 m
Mean Annual Air Temperature	7.2°C
Mean Yearly Surface Temperature (Semi-rigid Section)	12.5°C
Mean Yearly Surface Temperature (Flexible Section)	12.4°C
Range Yearly Surface Temperature (Semi-rigid Section)	11.9°C
Range Yearly Surface Temperature (Flexible Section)	11.8°C
Range Daily Surface Temperature (Semi-rigid Section)	23.8°C
Range Daily Surface Temperature (Flexible Section)	22.9°C
Number of Freezing Degree Days	420
Annual Rainfall	806 mm
Average Relative Humidity	81%
Average Wind Speed	3.5 m/s
Solar radiation Minimum	825 W/m^2
Solar radiation Maximum	10700 W/m^2

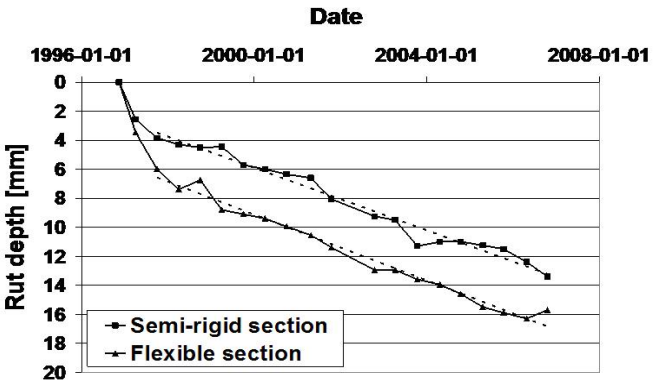

Fig. 10. Total Observed Rut Depth in the Semi-rigid and Flexible Test Sections.

Climate

The CalME climatic input data consisting of hourly surface temperature data were derived using the Enhanced Integrated Climate Model v3.0, called EICM [5]. The input data consisted of layer structure, material data, hourly climatic data (hcd) from the Swedish National Road Administration and the Swedish Meteorological and Hydrological Institute, and ground water from the Geological Survey of Sweden [26-28]. The two test sections were modeled separately since the results depend on the structure and thermal conductivity of the materials. The results were inserted directly into the CalME climate database file.

The climatic data time interval comprised January 2003 to February 2006. The ground water depth, calculated as the mean value of Halmstad and Oskarström [28], was constant throughout the year. The daily solar radiation maximum and sunrise/sunset times were modeled as a function of latitude [5]. Air temperature, wind speed and relative humidity were provided by hourly on-site measurements [26]. Precipitation was approximated by accumulated 6 h data from nearby Halmstad distributed hourly according to Helsingborg 1 h data. The percent of sunshine, i.e. absence of cloud cover, was approximated using Växjö data as that was the closest complete sunshine data set [27]. A summary of the EICM output data is provided in Table 7.

CalME Simulation Options

Regarding simulation options in the CalME software, the damage was calculated separately for each layer. Lateral wander was accounted for but moisture ingress and reflection cracking were excluded from the analysis. Ageing was continued throughout the

entire pavement life. The linear elastic response (LET) model was used with the 30 day default increment and the default day subdivision. The model was kept deterministic by using no variability.

Field Measurement

The transversal surface profile was measured twice per year, in April and October, from 1997 to 2006 using a PRIMAL transversal profilometer [29]. The total rut depth derived from measured profile data using the wire line method is shown in Fig. 10. However, during winter Swedish asphalt pavements exhibit considerable wear rutting due to studded tires [29], while CalME currently does not consider this distress mechanism. Therefore, the measured total rut depth data were adjusted for wear rutting using additional laser profilometer mea resusurements [29]. This resulted in the rut depths presented in Fig. 11. The occasional flattening and reversal of rut depth growth can be attributed to scatter. The growth of permanent deformation appears linear after one year when the initial deformation has developed, as shown with the dotted line in both figures. Again, it should be noted that the specific sections selected for this study are not necessarily representative for the pavement structures and materials. Comparisons between observation and model results were carried out using all observation points in order to account for measurement variation.

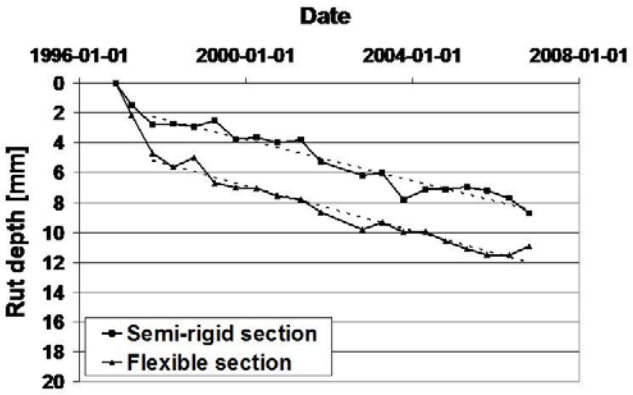

Fig. 11. Observed Rut Depth in the Semi-rigid and Flexible Test Sections Adjusted for Wear Rutting.

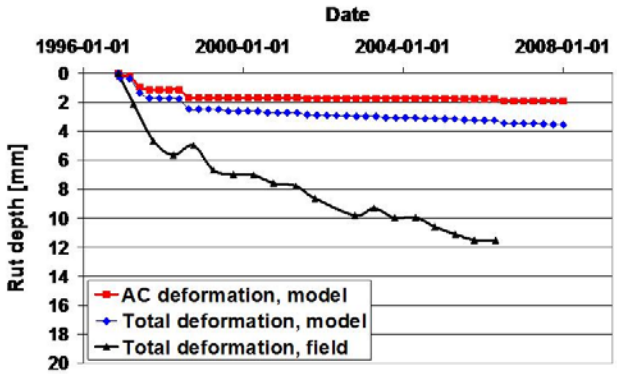

Fig. 12. Rut Depth in the Flexible Test Section Using Measured Permanent Deformation Parameters.

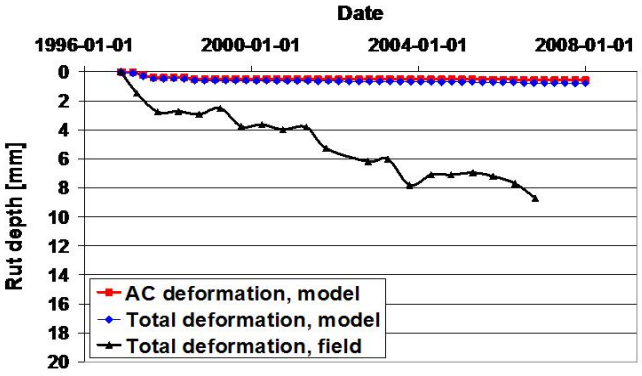

Fig. 13. Rut Depth in the Semi-rigid Test Section Using Measured Permanent Deformation Parameters.

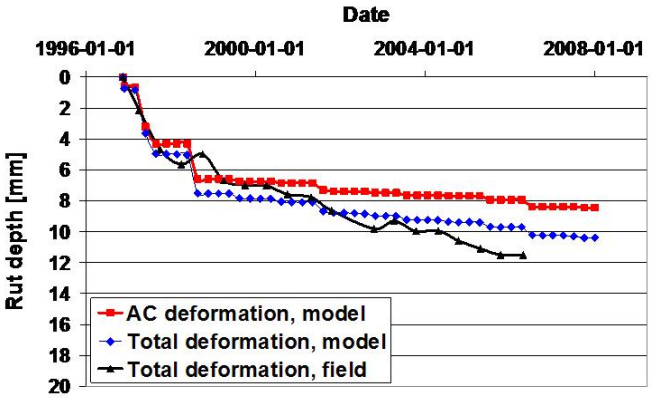

Fig. 14. Rut Depth in the Flexible Test Section Using WesTrack Permanent Deformation Parameters.

Results

The results from the simulations with measured and calculated mean WesTrack permanent deformation parameters are presented separately and compared with measured rut depth data. The total modeled rut depth and the modeled contribution from asphalt concrete (AC) layers are presented in each figure in this section of the paper. The difference between them is permanent deformation in unbound materials. The stiffness in each layer is also presented in addition to the resulting permanent deformations.

Permanent Deformation Using Measured Data

The CalME simulations carried out using measured permanent deformation data under-predicted total rut depth in both sections. The simulations with measured permanent deformation data in the flexible section accounted for only 28% of the rut depth after ten years of traffic, as shown in Fig. 12. Both the initial first-year deformation and the yearly growth of the total deformation were underestimated. The contribution of modeled asphalt concrete (AC) deformation to total modeled deformation was 55%, which was somewhat less than expected considering the thick asphalt layers [11]. In the semi-rigid section, the model accounted for only 9% of

the total rut depth after ten years as shown in Fig. 13. Further, the AC contribution to total modeled deformation was 73%. Almost all permanent deformation in the semi-rigid section was expected to occur in the asphalt concrete layers [11]. Contrary to the continuous field rutting growth, the modeled total rutting rate was negligible after the first year.

Permanent Deformation Using WesTrack Data

The CalME permanent deformation simulations corresponded well to the observed total permanent deformation in the flexible section but resulted in underestimation in the semi-rigid section. The CalME simulations carried out using WesTrack permanent deformation data in the flexible section accounted for a reasonable 84% of the rut depth after ten years of traffic, as shown in Fig. 14. Note that the first five years were modeled very accurately, but after that the yearly growth was somewhat underestimated. The contribution of modeled asphalt concrete (AC) deformation to total modeled deformation was 82%. In the semi-rigid section, the model accounted for only 32% of the total rut depth after ten years as shown in Fig. 13. Further, the AC contribution to total modeled deformation was 92%, which is expected due to thick bound layers [11]. Contrary to the continuous field rutting growth, the modeled total rutting rate was very small after the first year.

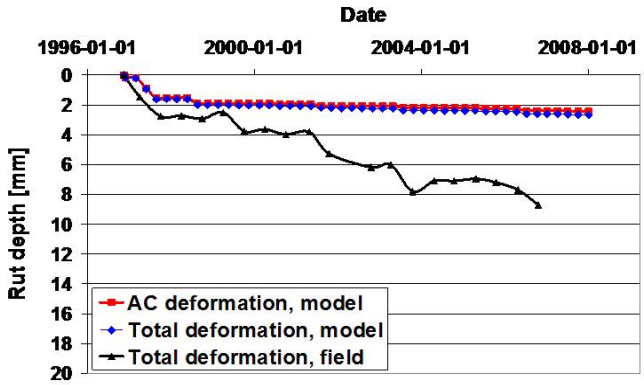

Fig. 15. Rut Depth in the Semi-rigid Test Section Using WesTrack Permanent Deformation Parameters.

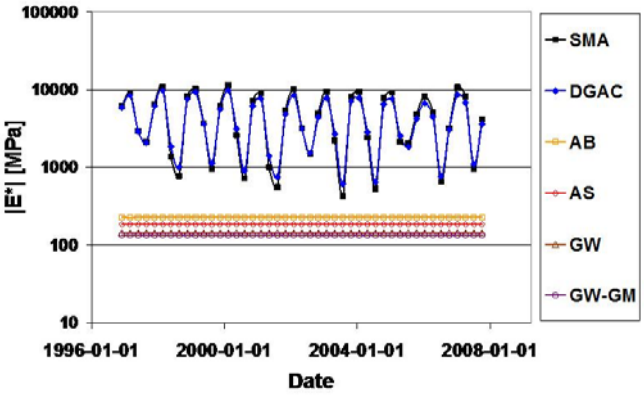

Fig. 16. Stiffnesses of the Flexible Section Layers.

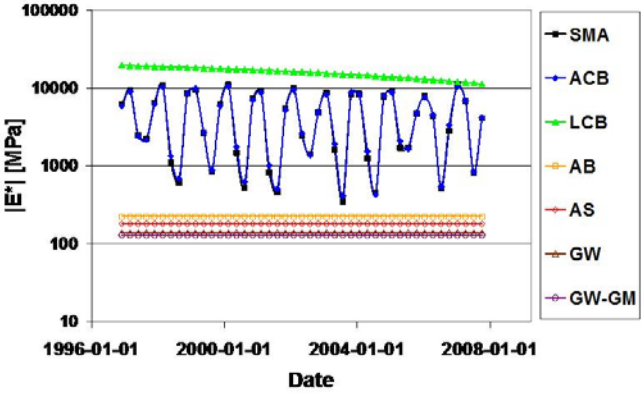

Fig. 17. Stiffnesses of the Semi-rigid Section Layers.

Layer stiffness

The modeled asphalt concrete stiffness showed an expected seasonal variation and a slight long-term decrease due to damage despite ageing in both the semi-rigid and flexible sections. The modeled mean stiffness reduction during the first five years was 8.7% for the stone mastic asphalt (SMA) layers, 10.2% for the dense-graded asphalt concrete (DGAC) layers and 6.9% for asphalt concrete base (ACB) layers, as illustrated in Fig. 16 and Fig. 17. The constant rate reduction of the lean concrete base (LCB) stiffness in the semi-rigid pavement section, shown in Fig. 17, was the expected result of the calibration using falling weight deflectometer data, as previously discussed. The stiffnesses of aggregate base (AB) and subbase (AS) layers were constant throughout the pavement life, as well as the well-graded gravel (GW) and well-graded/silty gravel (GW-GM) subgrade layers.

Discussion

Permanent Deformation Model

Measured and WesTrack Parameters

Comparison between CalME rut depth results using measured and estimated mean WesTrack permanent deformation parameters for asphalt concrete indicated that the relation between elastic and plastic properties is affected by ageing. The CalME methodology prescribes permanent deformation characterization using the repeated simple shear test at constant height (RSST-CH) performed with newly compacted specimens. The RSST-CH test data is processed into a permanent deformation parameter set, which is a measure of the relation between elastic and plastic properties of an asphalt concrete material. CalME assumes that the permanent deformation parameter set is constant throughout the pavement life, which theoretically leads to the possibility of determining the parameter set using aged specimens. In this case, CalME seriously underestimated rut depth using input data produced with the RSST-CH and 12-years-old specimens, while CalME simulations with mean WesTrack data resulted in good predictions. This means that ageing appears to have an influence on the RSST-CH results, i.e. the relation between plastic and elastic strain, assuming that CalME would have predicted rut depth accurately if the material testing had

been performed on newly compacted field cores according to the original CalME methodology. Therefore, the results from a limited number of specimens indicate that the RSST-CH parameters may be dependent on the asphalt concrete layer age. The ageing dependency of the plastic-elastic relation should be further investigated.

The reduction of permanent deformation due to the use of aged RSST-CH specimens mainly appeared to be caused by a reduction of the dependency on the number of loadings. The permanent deformation curve appearances of the RSST-CH were measured, and the mean WesTrack permanent deformation parameters are shown in Fig. 6, while the corresponding CalME rut depth results based on that data are shown in Figs. 12 to 15. Permanent deformation modeling with RSST-CH measured parameters showed some initial deformation and very small continuous growth, while the corresponding results using mean WesTrack data showed significant effects of both initial and continuous growth. That behavior should be compared with the field-measured rut depth,

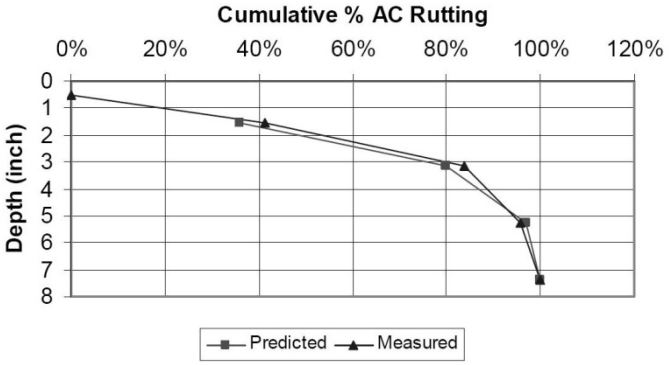

Fig. 18. AC Rutting as a Function of Depth [3].

which exhibited a small initial growth and a large continuous growth. The results indicate that the dependency of the number of loadings may be the main ageing effect, assuming that CalME would have predicted rut depth accurately if the RSST-CH testing had been performed on newly compacted field cores according to the original CalME methodology.

Flexible pavement section

The CalME modeled rut depth using mean WesTrack asphalt concrete permanent deformation parameters and observed rut depth showed good correlation, which was not entirely expected due to the CalME model structure. The CalME model assumes that the total flow rutting can be represented with the shear deformation 50 mm beneath the tire edge, and that it is proportional to layer thickness down to 100 mm depth. The CalME assumption that no flow rutting occurs below 100 mm depth appears reasonable based on the results of several studies. Trench studies carried out on flexible pavements in a wide range of US states showed that most of the rutting appeared in the top 76.1-101.6 mm (3-4 inches) of the AC layers [30]. Similar conclusions were reached using Heavy Vehicle Simulator (HVS) tests on multiple structures employing varying wheel configurations and temperatures [31]. In addition, the seven-section MnROAD trench study used for calibration of the Mechanistic-Empirical Pavement Design Guide (M-E PDG) showed that approximately 90% of the AC permanent deformations occurred in the top 100 mm [3], as illustrated in Fig. 18.

However, flow rutting in Swedish flexible pavement structures may be located deeper than in corresponding American pavements. Approximately one third of the total flow rutting appeared at 120-200 mm depth in the low-modulus asphalt concrete base (ACB) layers in a typical Swedish flexible pavement instrumented with vertical strain gauges in each layer and subjected to HVS loading [32]. The ACB layer in that study was made of 160/220 penetration bitumen in order to withstand cracks due to frost-heave and fatigue at the expense of permanent deformation resistance. The flexible pavement section in this study employed that same ACB material. This suggests that approximately one third of the permanent deformation could have occurred at depths greater than what CalME considers. Therefore, it was not certain that the CalME model would account for all permanent deformations in the 222 mm thick asphalt concrete layers of the flexible pavement section in this study. Nevertheless, CalME rut depth results using WesTrack permanent deformation parameters correlated well with observed rut depths. This could mean that the ACB layer deformation was located in the top 65 mm, directly below the 35 mm stone mastic asphalt (SMA) wear layer. In order to further investigate the matter, the authors suggest that the CalME materials library be expanded with various types of materials and structures.

Semi-rigid pavement section

The underestimation of permanent deformation in the semi-rigid pavement section was not expected, although it should be noted that semi-rigid pavements were not included in the CalME calibration efforts. Both measured and WesTrack permanent deformation parameters underestimated the total rut depth. The previously discussed AC permanent deformation limitation at depths larger than 100 mm could not significantly have affected the results as the AC layers were only 102 mm. The lack of permanent deformation observed in the unbound layers appears reasonable since lean concrete base (LCB) layers act as a stiff plate with great loading distribution capability.

The modeled flow rutting in the semi-rigid section was approximately a third of that modeled in the flexible section, which is notable since their AC permanent deformation parameters were similar, as illustrated in Fig. 16. Further, the observed flow rutting was only slightly less in the semi-rigid section. However, it should be noted that the permanent deformation parameters only determine the relation between elastic and plastic shear strains. Therefore, the elastic strains at 50 mm depth must have been much lower in the semi-rigid pavement section than in the flexible. The small elastic strains in the semi-rigid layer are most likely due to the very stiff LCB layer. The underestimation of rut depth in the semi-rigid section suggests that the shear stress and elastic shear strain at 50 mm depth may be difficult to relate to flow rutting in very stiff pavement sections.

Asphalt concrete layer stiffness

The asphalt concrete minimum dynamic modulus assumption of 100-200 MPa appears reasonable in the context of the CalME model. Modeling the minimum dynamic modulus accurately is important

considering that the potential for permanent deformation in asphalt concrete is high when the dynamic modulus is low. Determining the mastercurve parameters based on laboratory test data is difficult as many solutions often appear to fit measured data equally well. Low modulus measurements are carried out at high temperatures and/or low frequencies, which may cause excessive permanent deformation and yield unreliable data. Further, laboratory tests have been found to result in a significantly lower minimum dynamic modulus than practical field measurements using the falling weight deflectometer (FWD) [8]. The difference is explained by the stiffening boundary conditions applied in the field compared to those of a detached specimen in a laboratory test. For the reasons above, it appears appropriate to use some minimum dynamic modulus assumption. The value recommended by CalME manual is 100-200 MPa based on the modulus of the aggregate alone [4]. However, considering its high impact on permanent deformation, the minimum dynamic modulus assumption should be further investigated.

The slight long-term dynamic modulus reduction due to damage despite the ageing effect was not entirely expected. CalME has the advantage of adjusting the asphalt concrete stiffness according to both damage and ageing, which are governed by separate functions. In California, the net effect is often an overall reduction in FWD measured dynamic modulus [8]. However, damage is caused by the traffic volume, which is considerably lower in Sweden. The mean initial number of heavy axles per lane and year was 3.4 million on roads in the CalME WIM database, compared to 1.1 million on the Swedish E6 motorway. A follow-up study was carried out on nearby pavement sections theoretically identical to those in this study [33]. The cores were obtained from one of the wheel tracks, i.e. they were subjected to both ageing and damage caused by repeated traffic loadings. They were tested using the repeated diametral loading tests at +10°C according to FAS Method 454 [34]. During the first five years, their stiffness increased by 18%, 38% and 69% for the stone mastic asphalt (SMA), the dense-graded asphalt concrete (DGAC) and the asphalt base layers (ACB), respectively. On the contrary, CalME showed a corresponding stiffness reduction of 8.7% for the SMA, 10.2% for the DGAC layers and 6.9% for the ACB, as reported in the results section.

Two interpretations are possible to explain the above difference in stiffness results, considering that the overall stiffness is continuously increased by ageing and reduced by damage. The stiffness increase could have been underestimated by the predetermined ageing function according to Swedish specifications [13]. Alternatively, the CalME damage function with mean WesTrack asphalt concrete parameters could have overestimated the damage for the asphalt concrete layers in this study. These results underline the general need for using measured ageing and damage data, and that any estimated data should be based on materials of similar composition. Therefore, CalME is recommended to further develop the ageing and damage functions and to expand their materials library.

Conclusions

Based on the results of this paper, the following conclusions were drawn:

- The relation between plastic and elastic shear properties, measured with Repeated Simple Shear Test at Constant Height on a limited number of specimens, appeared to be affected by ageing. The suggested main ageing effect was loss of dependency on the number of loadings. The ageing dependency of the RSST-CH parameters should be further investigated.
- The CalME model rut depth prediction correlated well with observations in the flexible pavement section using default mean WesTrack permanent deformation data.
- The results from the semi-rigid pavement section indicate that shear stress and elastic shear strain may be difficult to relate to flow rutting in very stiff pavement sections. Semi-rigid pavement sections should be included in the re-calibration process.
- The CalME 100-200 MPa minimum dynamic modulus assumption for asphalt concrete, based on falling weight deflectometer data, should be further investigated.
- The advanced CalME asphalt concrete stiffness models for ageing and damage should be further developed and calibrated and the CalME materials library should be expanded.

Acknowledgements

The financial support provided by the Swedish National Road Administration (SNRA) and the Development Fund of the Swedish Construction Industry (SBUF) is gratefully acknowledged. The authors wish to thank the staff at the Pavement Research Center at University of California, Berkeley, for their support, and especially John Harvey, Erik Denneman and Frank Farshidi for their guidance and fruitful discussions on CalME. The paper also benefitted from advice from Safwat Said at the Swedish National Road and Transport Research Institute (VTI), Monica Berntman at Lund University and Richard Nilsson at Skanska Teknik.

References

1. Pavement Research Center, (2009). *CalME v0.82 software*, Institute of Transportation Studies, University of California, Davis, California, USA.
2. Caltrans, (2008). Flexible Pavement: Chapter 630, *Caltrans Highway Design Manual*, California Department of Transportation, Sacramento, California, USA.
3. NCHRP, (2004). Guide for the Mechanistic-Empirical Design of New and Rehabilitated Pavement Structures, *NCHRP Report 1-37A*, Transportation Research Board, Washington, D.C., USA.
4. Pavement Research Center, (2008). *Software documentation for CalME v0.8*, Institute of Transportation Studies, University of California, Davis, California, USA.
5. Larson, G.E. and Dempsey, B.J., (2003). *Enhanced integrated climate model (EICM) v3.0*, Applied Research Associates, ERES Division, Columbia, Maryland, USA; Department of Civil Engineering, University of Illinois, Champaign, Illinois, USA.
6. Monismith, C.L., Deacon, J.A., and Harvey, J.T., (2000). WesTrack: Performance Models for Permanent Deformation

and Fatigue, *Report to Nichols Consulting Engineers, Chtd.*, Pavement Research Center, Institute of Transportation Studies, University of California, Berkeley, California, USA.

7. Deacon, J.A., Harvey, J.T., Guada, I., Popescu, L., and Monismith, C.L., (2002). Analytically Based Approach to Rutting Prediction, *Transportation Research Record,* No. 1806, pp. 9-18.
8. Ullidtz, P., Harvey, J., Tsai, B.W., and Monismith, C., (2006). Calibration of Incremental-Recursive Flexible Damage Models in CalME Using HVS Experiments, *Report No. UCPRC-RR-2005-06*, Pavement Research Center, Institute of Transportation Studies, University of California, Berkeley and Davis, California, USA.
9. Ullidtz, P., Harvey, J., Tsai, B.W., and Monismith, C., (2006). Calibration of CalME models using WesTrack Performance Data, *Report No. UCPRC-RR-2006-14*, Pavement Research Center, Institute of Transportation Studies, University of California, Berkeley and Davis, California, USA.
10. Jones, D., Tsai, B.W., Ullidtz, P., Wu, R., Harvey, J., and Monismith, C., (2007). Reflective Cracking Study: Second-Level Analysis Report, *Report UCPRC-RR-2007-09 for Caltrans Division of Research and Innovation*, Pavement Research Center, Institute of Transportation Studies, University of California, Davis and Berkeley, California, USA.
11. Wiman, L.G., Hermelin, K., Ydrevik, K., Hultqvist, B.-Å., Carlsson, B., Viman, L., and Eriksson, L., (1997). Prov med olika överbyggnadstyper: Observationssträckor på väg E6, Fastarp-Heberg, *VTI notat 56:1-1997*, The Swedish National Road & Transport Research Institute, Linköping, Sweden (in Swedish).
12. Hermelin, K., (1997). Prov med olika överbyggnadstyper: Observationssträckor på E6, Fastarp-Heberg, *VTI notat 56:3-1997*, The Swedish National Road & Transport Research Institute, Linköping, Sweden (in Swedish).
13. Swedish National Road Administration, (2005). ATB Väg: General technical specifications for road structures, *Report 2005:112*, Swedish National Road Administration, Borlänge, Sweden (in Swedish).
14. Said, S.F., (2005). Ageing Effect on Mechanical Characteristics of Bituminous Mixtures, *Transportation Research Record*, No. 1901, pp. 1-9.
15. Kim, Y.R., Seo, Y., King, M., and Momen, M., (2004). Dynamic modulus testing of asphalt concrete in indirect tension mode, *Transportation Research Record*, No. 1891, pp. 163-173.
16. AASHTO, (2006). *T320-03: Standard Method of Test for Determining the Permanent Shear Strain and Stiffness of Asphalt Mixtures using the Superpave Shear Tester (SST), 2006 Edition*, American Association of State Highway and Transportation Officials, Washington, D.C., USA.
17. Wiman, L.G., Carlsson, H., Viman, L. and Hultqvist, B-Å. (2005). Prov med olika överbyggnadstyper: Observationssträckor på väg E6, Fastarp-Heberg, Resultatrapport efter 7 års uppföljning, 1996-2003, *VTI notat 25-2005*, The Swedish National Road & Transport Research Institute, Linköping, Sweden (in Swedish).
18. Swedish National Road Administration, (1994). Väg 94: General technical specifications for road structures, *Report 1994:26*, Swedish National Road Administration, Borlänge, Sweden (in Swedish).
19. Swedish National Road Administration, (2000). VVMB 114: Bearbetning av deflektionsmätdata, erhållna vid provbelastning av väg med FWD-apparat, *Report 2000:29*, Swedish National Road Administration, Borlänge, Sweden (in Swedish).
20. Swedish National Road Administration, (2008). *WIM data from Kungsbacka 13-536 southbound 2004 and Löddeköpinge M482 southbound 2005-2007*, Swedish National Road Administration, Borlänge, Sweden (in Swedish).
21. Lu, Q., Harvey, J., Le, T., Lea, J., Quinley, R., Redo, D., and Avis, J., (2002). *Truck Traffic Analysis using Weigh-In-Motion (WIM) Data in California*, Pavement Research Center, Institute of Transportation Studies, University of California, Berkeley, California, USA.
22. Swedish National Road Administration, (2008). Data points 454 and 9454 in traffic flow web database, *Kartor med trafikflöden, Klickbara kartan*, Swedish National Road Administration, Borlänge, Sweden, Last Accessed May, 2008 (in Swedish).
23. European Asphalt Pavement Association, (1995). *Heavy duty pavements: The arguments for asphalt*, European Asphalt Pavement Association, Breukelen, the Netherlands.
24. Sebaaly, P.E., (2003). Determination of Pavement Damage from Super-single and Singled-out Dual Truck Tires, *NCHRP Report 1-36*, Transportation Research Board, Washington, D.C., USA.
25. Buiter, R., Cortenraad, W.M.H., van Eck A.C., and Van Rij, H., (1989). Effects of transverse distribution of heavy vehicles on thickness design of full-depth asphalt pavements, *Transportation Research Record*, No. 1227, pp. 66-74.
26. Swedish National Road Administration, (2008). *Climate data from VViS station No. 1336*, Swedish National Road Administration, Borlänge, Sweden.
27. Swedish Meteorological and Hydrological Institute, (2008). *Swedish meteorological data 1996-2008*, Swedish Meteorological and Hydrological Institute, Norrköping, Sweden.
28. The Geological Survey of Sweden, (2008). *Ground water depth data from Halmstad and Oskarström 1998-2008*, The Geological Survey of Sweden, Uppsala, Sweden.
29. Wiman, L.G., Carlsson, H., Viman, L., and Hultqvist, B.-Å., (2009). Prov med olika överbyggnadstyper: Uppföljning av observationssträckor på väg E6 Fastarp-Heberg, 10-årsrapport, 1996-2006, *VTI Rapport 632-2009*, The Swedish National Road & Transport Research Institute, Linköping, Sweden (in Swedish).
30. Brown, E. R. and Cross, S. A., (1992). A National Study of Rutting in Hot Mix Asphalt (HMA) Pavements, *NCAT Report 92-5*, National Center for Asphalt Technology, Auburn, Alabama, USA.
31. Harvey, J. and Popescu, L., (2000). Rutting of Caltrans Asphalt Concrete and Asphalt-Rubber Hot Mix under Different Wheels, Tires and Temperatures – Accelerated Pavement Testing Evaluation, *Draft report submitted to the California Department of Transportation*, Pavement Research Center, Institute of Transportation Studies, University of California,

Berkeley, California, USA.
32. Oscarsson, E., (2007). Prediction of Permanent Deformations in Asphalt Concrete using the Mechanistic-Empirical Pavement Design Guide, *Licentiate's Thesis. Bulletin 236*, Department of Technology and Society, Lund University, Lund, Sweden.
33. Wiman, L.G., Hermelin, K., Ydrevik, K., Hultqvist, B.-Å., Carlsson, B., Viman, L., and Eriksson, L., (2002). Prov med olika överbyggnadstyper: Observationssträckor på väg E6, Fastarp-Heberg, Resultatrapport efter 5 års uppföljning, 1996-2001, *VTI notat 52-2001*, The Swedish National Road & Transport Research Institute, Linköping, Sweden (in Swedish).
34. Swedish Asphalt Pavement Association, (1998). *FAS Method 454-98*, Swedish Asphalt Pavement Association, Stockholm, Sweden (in Swedish).